Available online at www.sciencedirect.com
SCIENCE DIRECT
Journal of Photochemistry and Photobiology A: Chemistry 180 (2006) 271–276
Journal of Photochemistry and Photobiology A:Chemistry
www.elsevier.com/locate/jphotochem

Classical aspects emerging from local control of energy and particle transfer in molecules

Stefanie Gräfe, Philipp Marquetand, Volker Engel *

Institut für Physikalische Chemie, Am Hubland, 97074 Würzburg, Germany

Available online 28 February 2006

This work is dedicated to Prof. Volker Staemmler on the occasion of his 65th birthday.

Abstract

The question in how far classical mechanics can be used to describe coherent control processes in molecules is addressed within the framework of local control theory. Therefore, quantum and classical calculations are compared for a model proton transfer process and also for the multi-photon infrared dissociation of the HOD molecule. It is shown that control fields can be derived classically as long as wave packet dispersion is not too large. This hints at further applications which might be helpful to devise control fields for complex molecular systems being present in biological processes.

Keywords: Coherent control; Molecular dynamics; Quantum dynamics; Proton transfer; Photo fragmentation

1. Introduction

Elementary processes in chemistry and biology follow fundamental physical laws. The motion of electrons and nuclei and their interaction with electromagnetic fields, in general, have to be described employing the concepts of quantum mechanics and quantum electrodynamics. In many cases, however, a quantization of the external fields is not necessary and the latter may be implemented in their classical form. Moreover, a treatment of the particle motion within the frame of classical mechanics is often sufficient. This, actually, is a common approach in theoretical biology and chemistry if dealing with complex systems: solving the classical equations of motion, combined with statistical averaging, is at the heart of molecular dynamics (MD) simulations [1,2]. The present issue of this journal is concerned with the control of chemical and biological reactions [3–7] with the help of ultrashort pulses of radiation, commonly obtained from modern laser light sources [8]. The concept of coherence is of central significance here. Coherent light has the property to produce interference, for a detailed discussion and more specific definition of coherence see the classical text by Born and Wolf [9]. Employing such fields, it is then possible to transfer coherences into a quantum system. As time goes along, the system might feel fluctuations introduced by a surrounding bath so that the fixed phases, now present in the quantum mechanical wave functions, are disturbed. It is to be noted, however, that this destruction of coherence relies on an arbitrary separation of the world into a sub-quantum system and a bath.

The possibility of interference is not included if one regards particles, i.e. atoms bound together in molecules, as classical objects. In the spirit of what has been said above, this suggests that a classical description of coherent control processes, relying on wave-like properties, is not possible. Thus we are faced with a dilemma: on one hand, the treatment of complex molecules is only feasible employing the classical equations of motion (if all interactions are known sufficiently accurate), and on the other hand, 'coherent control' needs a quantum description. As a consequence, it seems not to be possible to find a consistent theoretical approach for the treatment of control processes in complicated systems. In this paper it is shown that this, in general, might be a too pessimistic point of view. Employing model systems, it is demonstrated that the pulses needed to perform a certain task can be derived, within limits, from classical trajectories. In order to arrive at some reliable results, classical and quantum calculations are contrasted for the case of a proton transfer in a two-mode system, and also for the infrared

* Corresponding author. Tel.: +49 931 888 6376.
E-mail address: voen@phys-chemie.uni-wuerzburg.de (V. Engel).

1010-6030/$ – see front matter © 2006 Elsevier B.V. All rights reserved.
doi:10.1016/j.jphotochem.2006.01.015

dissociation of the HOD molecule. These studies are undertaken with the hope that, if the limitations of a classical treatment are characterized in the treatment of smaller model systems, applications to larger molecules can be judged on these grounds.

The methodology employed below is that of 'local control' [10–13]. Within this approach it is the system's dynamics which determines the control field at any instant of time. This enables us to get an insight into the relation between the dynamics and the properties of the field [14,15]. This approach is related to what is known as *tracking* of *inverse control* [16,17] but is somehow simpler in its formulation.

The paper is organized as follows: the strategy of 'local control' is outlined in Section 2. Numerical results are contained in Section 3, and a summary is given in Section 4.

2. Local control theory: quantum and classical approach

In the examples treated below, the reactive processes are initiated by an energy transfer between molecules and an external electric field. Within the quantum approach, the Hamilton operator $H(t)$ consists of a part H_0 belonging to the unperturbed molecule and a dipole-perturbation term $W(t)$ which includes the interaction with the classical field:

$$H(t) = H_0 + W(t) = (T(P) + V(R)) - \mu(R)E(t). \tag{1}$$

Here, $T(P)$ denotes the kinetic energy operator depending on the momentum operators (P) of all particles. The coordinates entering into the potential energy expression $V(R)$ are abbreviated as (R). Furthermore, $\mu(R)$ is the projection of the dipole moment on the polarization vector of the field, and $E(t)$ describes the time-dependence of the latter.

The efficiency of the field-molecule energy transfer is characterized by a rate calculated as the time-derivative of the expectation value of H_0:

$$\frac{\mathrm{d}}{\mathrm{d}t}\langle H_0\rangle_t = \frac{\mathrm{d}}{\mathrm{d}t}\langle\psi(t)|H_0|\psi(t)\rangle = \frac{\mathrm{i}}{\hbar}\langle[H, H_0]\rangle_t, \tag{2}$$

where the time-dependent Schrödinger equation for the wave function $\psi(t)$ is used in deriving the last equality. The commutator $[H, H_0]$ appearing in the rate expression is readily evaluated, yielding

$$\frac{\mathrm{d}}{\mathrm{d}t}\langle H_0\rangle_t = \frac{\mathrm{i}}{\hbar}E(t)\langle[T(P), \mu(R)]\rangle_t. \tag{3}$$

This is the central equation which is employed below to control various processes in molecules: because the field $E(t)$ appears in the rate expression, it may (in principle) be chosen to yield a positive rate amounting to a net absorption of energy by the system (this will be called 'heating', in what follows). Alternatively, it can be determined in a way that the rate is negative, leading to an energy loss ('cooling') of the system.

The connection between the quantum dynamics and a control field being able to induce heating or cooling is most easily established in the case of the one-dimensional motion of a particle with mass m, where the dipole moment is assumed to be a linear function of a single coordinate ($\mu(R) = \mu_0 + \mu_1 R$). In this case one obtains

$$\frac{\mathrm{d}}{\mathrm{d}t}\langle H_0\rangle_t = \frac{\mu_1}{m}E(t)\langle P\rangle_t. \tag{4}$$

Thus, the rate is proportional to the expectation value of the momentum operator. As a result, if the field is chosen to be in phase with the mean momentum, energy is pumped into the system. On the other hand, if it is determined to be out of phase with $\langle P\rangle_t$, energy is taken away from the system.

Next, we turn to a classical treatment of the driven oscillator with the Hamilton function

$$\begin{aligned} H(t) &= \frac{(P(t))^2}{2m} + V(R(t)) - \mu(R(t))E(t) \\ &= H_0(t) - (\mu_0 + \mu_1 R(t))E(t), \end{aligned} \tag{5}$$

where now, $R(t)$ and $P(t)$ denote position and momentum, respectively. The energy rate is then evaluated taking Hamilton's equations of motion into account:

$$\frac{\mathrm{d}}{\mathrm{d}t}H_0(t) = \frac{\mu_1}{m}E(t)P(t). \tag{6}$$

This result is the classical equivalent of the quantum expression Eq. (4) and it leads to identical conclusions concerning the relation between driving field, dynamics and energy transfer.

From the above equations one might conclude that, under certain circumstances, a quantum and classical derivation of control fields (within the frame of local control theory) might lead to similar fields. In how far this conclusion is possibly true is explored in the next section.

3. Results

3.1. Particle transfer

As a first example, the transfer of a particle with proton mass m is treated. Intramolecular or intermolecular proton (or hydrogen) transfer are extremely important elementary steps in many chemical reactions [18–20]. Within a simplified model, we treat a system with two degrees of freedom x and y, where the potential surface exhibits two minima. The potential is parameterized as follows:

$$V(x, y) = \Delta + ax^4 + b(y^2 - x^2) + cxy, \tag{7}$$

with the coefficients $\Delta = 0.220\,\mathrm{eV}$, $a = 6.940 \times 10^{-3}\,\mathrm{eV\,\AA^{-4}}$, $b = 7.774 \times 10^{-2}\,\mathrm{eV\,\AA^{-2}}$, and $c = 9.717 \times 10^{-3}\,\mathrm{eV\ \AA^{-2}}$ (the potential is constructed in atomic units and only after conversion the values of these parameters take the somehow strange values). The dipole moment is taken as a linear function in both degrees of freedom: $\mu(x, y) = x + y$ (in atomic units).

Fig. 1 displays contour lines of the potential surface. Two potential minima are clearly distinguishable which are separated by a barrier of ~0.22 eV. As an initial condition, the particle is localized in the well at positive values of the reaction coordinate x. This is simulated in choosing an initial wave function resembling the ground state of a Hamiltonian with a potential having only the single well occurring at positive distances x.

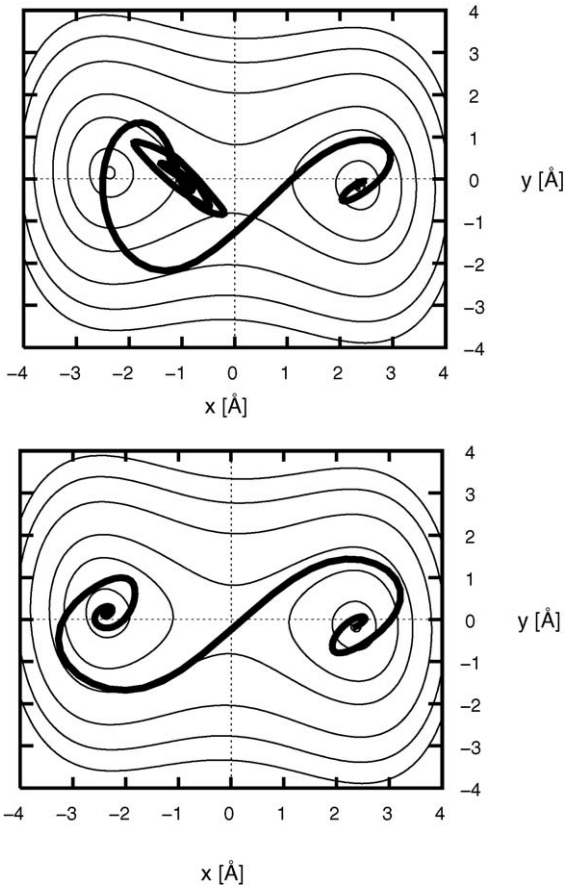

Fig. 1. Model system for a proton transfer. Shown are contours of the potential energy surface with energy values of (in eV) 0.0027, 0.0272, 0.1360, 0.2721, 0.5442, 0.8163, 1.088. The upper panel shows the time-dependent coordinate expectation value obtained from a quantum calculation. This orbit starts at the position of the initial wave packet in the right hand potential well. Upon interaction with the control field, the packet is transferred over the barrier and trapped in the region left of the dividing line at $y = 0$. The final time of the orbit is 1 ps. Lower panel: a single classical trajectory which is transferred by the classically determined field.

The objective of the control process is to move the particle over the barrier and localize it in the other potential well. Because we regard times for which tunneling – taking place on a much longer time-scale – can be neglected, this is only possible if energy is transferred into the system by a heating field. Upon absorption of sufficient energy, the particle might, eventually, cross the barrier and reach the region of the second potential minimum (at negative values of the reaction coordinate x). In order to stabilize the system one then needs a cooling field diminishing the particle's energy. Such a combination of heating and cooling fields is realized as follows. Starting from the quantum rate expression in the two-dimensional system

$$\frac{\mathrm{d}}{\mathrm{d}t}\langle H_0\rangle_t = \frac{1}{m}E(t)(\langle P_x\rangle_t + \langle P_y\rangle_t), \tag{8}$$

the field is determined as

$$E(t) = \lambda(\langle P_x\rangle_t + \langle P_y\rangle_t), (\langle x\rangle_t > 0),$$
$$E(t) = -\lambda(\langle P_x\rangle_t + \langle P_y\rangle_t), (\langle x\rangle_t < 0), \tag{9}$$

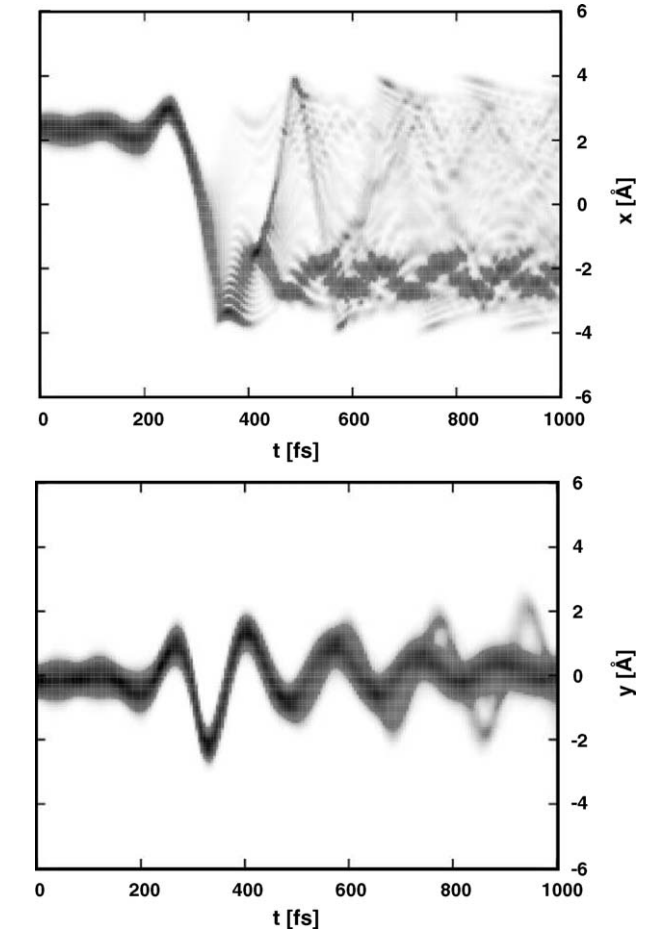

Fig. 2. Time-dependent quantum mechanical densities as a function of the reaction coordinate $\rho(x, t)$ (upper panel) and as a function of the additional vibrational mode $\rho(y, t)$ (lower panel).

where $\langle x\rangle_t$ denotes the expectation value of the reaction coordinate. This choice ensures that, if the wave packet is localized at positive values of x, the energy rate is positive (heating), whereas if it has moved over the barrier, a cooling is performed. The parameter λ is introduced to be able to vary the field strength.

The results of the quantum mechanical calculation (for $\lambda = 4 \times 10^{-4}$ a.u.) are contained in Fig. 1, upper panel. There, the thick black line shows the time evolution of the expectation value of the position vector $\vec{R}_{\mathrm{qm}}(t) = (\langle x\rangle_t, \langle y\rangle_t)$, where the starting point is around $\vec{R}_{\mathrm{qm}}(t = 0) = (2.5, -0.2)$ Å . In the figure, the time reaches up to 1000 fs. It can be seen that a vibrational motion in the initially occupied potential well is induced. This is followed by a barrier crossing and a motion confined to negative values of x. Note that this 'quantum trajectory' does not end up close to the minimum of the target potential well which is due to the fact that the transfer is not achieved to a 100%. This is illustrated in Fig. 2 which displays the densities

$$\rho(x, t) = \int \mathrm{d}y|\psi(x, y, t)|^2,$$
$$\rho(y, t) = \int \mathrm{d}x|\psi(x, y, t)|^2. \tag{10}$$

The reaction coordinate density $\rho(x, t)$ (upper panel) shows nicely the heating process which induces a vibrational motion, and also the barrier crossing around 300 fs. Afterwards, during the cooling process, most of the density is trapped at negative values of x. There is, however, a smaller fraction of density which becomes de-localized over the entire range of x between −4 and 4 Å. From the lower panel in Fig. 2 which contains the density $\rho(y, t)$ it is obvious, that the heating also triggers a vibrational motion in the direction perpendicular to the reaction coordinate. Indications can be found that a bifurcation of the density takes place, where one main part becomes restricted to positions close to $y = 0$, and another part performs a larger amplitude motion. Altogether, the calculation shows that the objective of particle transfer can be realized by the local control field – although, for the present set of parameters, does not result in a 100% yield.

Let us now turn to the classical approach to the problem. Therefore, a classical trajectory is started with zero momentum at the quantum mechanically determined value $\vec{R}_{\mathrm{qm}}(t = 0)$. The control field is derived from Eq. (9), where the expectation values are replaced by the canonical momenta $P_x(t)$ and $P_y(t)$, and the same value of the strength parameter λ as used in the quantum simulation is employed. In Fig. 1, lower panel, the classical position vector $\vec{R}_c(t) = (x(t), y(t))$ is shown. A comparison to the quantum case (upper panel) shows that the heating and barrier crossing proceeds almost identical. It is only at later times, that deviations are seen. In particular, the trajectory is forced to end up at the bottom of the target potential well. The reason is that only a single trajectory is taken into account and thus, because the lack of dispersion (an ensemble of orbits starting with different initial conditions are driven differently by a single field, see below), the transfer yield is always a 100%. Nevertheless, the quantum dynamics seems to be very much in accord with the classical motion, in the average. This point is strengthened if the control fields derived from the quantum expression (Eq. (9)) and its classical counterpart are compared. The latter are shown in Fig. 3, as indicated. For times before the barrier crossing, they are almost indistinguishable, tracking the momentum change in the system. When the crossing occurs, the fields exhibit a phase jump reflecting the switching from the heating to the cooling condition. At later times, the fields start deviating from each other, however, this difference is not dramatic. Thus, in the present example, control fields indeed can be constructed employing the laws of classical mechanics.

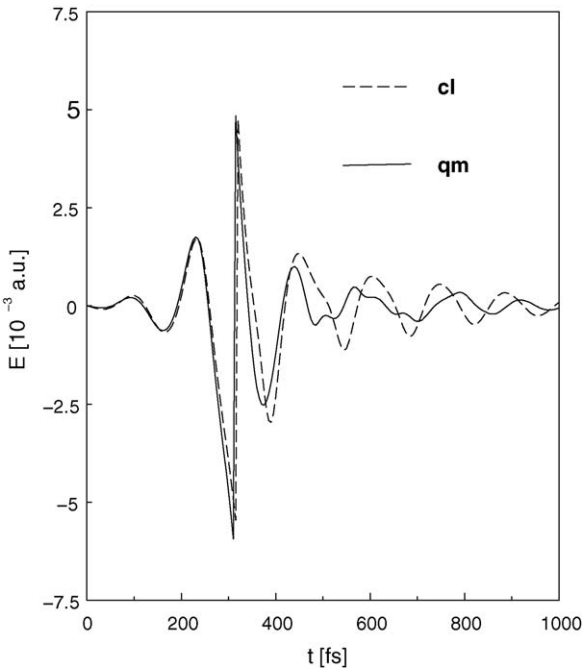

Fig. 3. Comparison of control fields derived from a quantum (qm) and a classical (cl) calculation, as indicated.

3.2. Energy transfer and dissociation

A photochemical process, where the absorption of photons leads to the breaking of a specific bond, serves as a second example. The photo dissociation of water in the first absorption band is one of the best understood processes in molecular physics [21,22]. Combining ultraviolet and infrared (IR) fields, several studies reported on the possibility to control the branching ratio of OH versus OD products originating from the HOD molecule [23,24]. In what follows, we exclude optical transitions and restrict our calculations to IR transitions within the ground electronic state of HOD. The molecule is assumed to be fixed in the xz-plane, where the z-axis bisects the bending angle which is kept constant at its equilibrium distance. The field is assumed to be polarized along the z-axis so that it equally couples to the two bonds. The potential surface and dipole moment function depending on the two distances R_{H} and R_{D} are taken from Refs. [23,25,26]. We employ the 'light-heavy-light approximation', where the oxygen mass is set to infinity, so that no kinetic coupling terms are present in the Hamiltonian [27].

In order to find an expression for a control field which is able to break one or the other bond, we impose the condition that the kinetic energy associated with the respective degree of freedom increases, in the average (alternatively one could start from expression (2), see Ref. [15]). Let us, in what follows, concentrate on the selective population of the D + OH channel. The rate is evaluated as

$$\frac{\mathrm{d}}{\mathrm{d}t}\langle T(P_{\mathrm{D}})\rangle_t = \frac{\mathrm{i}}{\hbar}E(t)\langle[T(P_{\mathrm{D}}), \mu(R_{\mathrm{H}}, R_{\mathrm{D}})]\rangle_t. \tag{11}$$

Here, m_{D} and P_{D} are the mass and momentum operator associated with the D atom. In the present case, the dipole moment is not a linear function of the coordinates [23], so that the expectation value of the commutator is evaluated at each time step. The control field is constructed as

$$E(t) = -\lambda\Im\langle[T(P_{\mathrm{D}}), \mu(R_{\mathrm{H}}, R_{\mathrm{D}})]\rangle_t, \tag{12}$$

where $\Im$ denotes the imaginary part of the complex (in fact, purely imaginary) number. This choice ensures, for a positive value of the strength parameter λ, that the rate (Eq. (11)) is positive at all times.

The classical equivalent of the rate expression can be obtained by using the correspondence

$$\{T(P_{\mathrm{D}}), \mu(R_{\mathrm{H}}, R_{\mathrm{D}})\} = -\frac{\mathrm{i}}{\hbar}[T(P_{\mathrm{D}}), \mu(R_{\mathrm{H}}, R_{\mathrm{D}})], \tag{13}$$

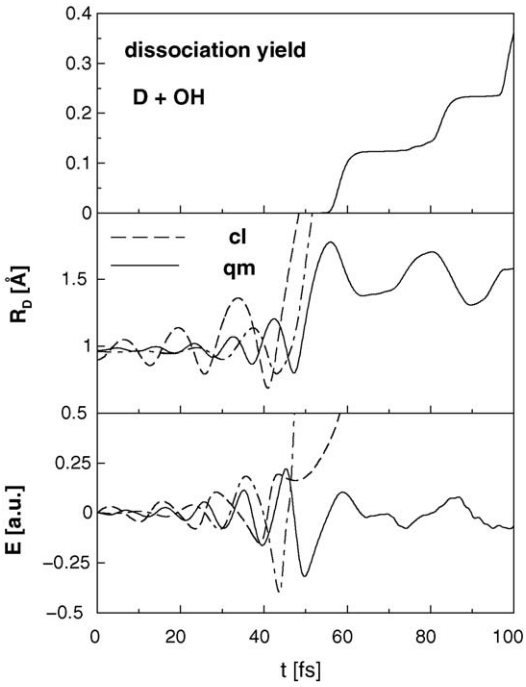

Fig. 4. Selective control of HOD fragmentation. The upper panel shows the (quantum) dissociation yield in the D + OH channel; the respective yield in the H + OD channel is zero. Middle panel: the quantum mechanical expectation value $\langle R_D \rangle_t$ is compared to two classical trajectories $R_D(t)$ which differ in their initial condition and also follow from fields with different strength parameters. The lower panel contains control fields constructed within a quantum mechanical (solid line) and classical (long dashed and dashed-dotted lines) treatment.

which relates the classical Poisson brackets $\{,\}$ to the quantum mechanical commutator [28]. The rate expression then reads

$$\frac{\mathrm{d}}{\mathrm{d}t} T(P_D)(t) = \frac{1}{m_D} E(t) P_D(t) \frac{\partial \mu(R_H, R_D)}{\partial R_D}. \quad (14)$$

This quantity assumes only positive values for the choice

$$E(t) = \lambda P_D(t) \frac{\partial \mu(R_H, R_D)}{\partial R_D}, \quad (15)$$

with λ, being a positive strength factor.

In Fig. 4 the quantum mechanically obtained dissociation yield in the D + OH channel is shown in the upper panel, where a value of $\lambda = 0.2$ a.u. is used in determining the control field. The yield is calculated from the norm of the wave packet which exits into the fragmentation channel and is localized at values larger than $R_D = 2.5$ Å. It is seen that the curve starts deviating from zero after about 50 fs and increases in steps. This can be understood in regarding the bond-length expectation value $\langle R_D \rangle_t$ which is shown in the middle panel of the figure as a solid line. In calculating this curve only the still bound parts of the wave packet are taken into account. The initial wave function is the ground state of the system and it takes some time until a vibrational motion is detectable, showing an increase in the oscillation amplitude. After 50 fs, the energy of the system has increased sufficiently, so that a first fraction of the wave packet is able to reach the continuum. At later times, the heating proceeds and additional parts of probability density enter into the exit channel. It is noted that for the present choice of parameters the yield of D + OH fragment is about 60% (obtained at long times) and that the excitation process is perfectly selective because no H + OD reaction products are built.

The figure also shows the classical position $R_D(t)$ (long dashed line) obtained for a value of $\lambda = 0.03$ a.u. used in Eq. (15). The trajectory is started with zero momentum at $R_H(0) = R_D(0) = 0.9$ Å. It is seen, that here the energy absorption proceeds faster than in the quantum case leading to an earlier D + OH dissociation. This is not due to intensity differences in the control fields as can be taken from the lower panel of Fig. 4. The amplitudes of the classically (long dashed line) and quantum mechanically derived field (solid line) are comparable but a phase shift is visible. Here, the interval below 50 fs should be regarded because afterwards dissociation sets in so that the trajectory leaves into the exit channel, whereas the wave packet shows a bifurcation into a bound and continuum part.

It is clear that a single trajectory can mimic the quantum dynamics only to a certain extent (a case where this is indeed possible was presented in the last subsection). In order to investigate the sensitivity of the results with respect to the choice of the initial conditions, another classical trajectory is started at $R_H(0) = R_D(0) = 0.96$ Å with zero momentum. The field strength parameter is set to $\lambda = 0.07$ a.u. so that the resulting control field strength is comparable to the one obtained from the quantum calculation (see lower panel of Fig. 4). The trajectory, displayed as a dashed-dotted line in the middle panel of the same figure shows a different oscillation period than the other orbit, as is to be expected. As a consequence it enters the exit channel at a different time which is close to the one where the first quantum wave packet is excited into the continuum. The dependence of the classically derived control fields on the initial conditions (lower panel) suggest that one should employ an ensemble of trajectories sampled from the initial quantum wave function [29] and calculate an average field to be then used in the quantum calculation. Nevertheless, even a single orbit yields a field which can serve as a sophisticated first guess for a field employed as input in, e.g., a feedback adaptive control procedure [30–33] realized in an experiment. For recent applications of adaptive control see, e.g. [34–38], or the reviews [5,7,39].

Deviations between the quantum and classical treatment are to be expected if a strong dispersion of the quantum mechanical wave packet is present. In this situation, the calculation of expectation values to be compared to their classical counterpart becomes meaningless [40]. It is to be noted, that even the quantum theory will not provide satisfactory results because the construction of the fields from local control theory rests on expectation values, for a discussion (and another numerical example) of the effect of delocalization see Ref. [41].

We finally mention that the oscillations of the average bond-length proceed with an increasing vibrational frequency which then is directly transferred into the field. Here, local control naturally leads to a field possessing a down chirp being necessary to achieve an effective ‘ladder climbing’ [42,43].

4. Summary

Local control theory is used to determine fields which are able to direct particle and energy transfer in molecules. In a first example, the proton transfer in a double well potential is regarded. There, the objective is to move the particle from one well to the other. It is shown, that this can be achieved quantum mechanically with a high efficiency. An analogous classical treatment yields the same dynamics and, in particular, the control field resulting from both theories are very similar. Here, the quantum wave packet remains rather localized so that the classical approximation is excellent. In particular, it has to be noted that the phase of the electric field can be derived classically. Thus, classical mechanics delivers a phase sensitive input for the control process.

A different situation is encountered in the second example considered, which is the photo fragmentation of the HOD molecule. Aiming at a preferential population of a single reaction channel, the quantum calculation shows that it is possible to exclusively populate the target channel. Although the same is obtained classically, the constructed fields differ to some extent. Here, it becomes clear that a careful sampling of initial conditions for the orbits is essential in order to be able to arrive at satisfactory results. Nevertheless, even in the case of a single orbit, the classical and quantum dynamics are similar so that a classically constructed field is still helpful as a first guess of how a control field should look like, in order to serve the predefined purpose.

Altogether, we believe that the potential of local control theory, i.e. its ability to connect quantum and classical dynamics, should be explored in more detail in order to arrive at a successful treatment of control problems in complex systems. Work along these lines is in progress.

Acknowledgment

Financial support by the Helmholtz/NRC program (project ADAM, ADAM2) is gratefully acknowledged.

References

[1] M.P. Allen, D.J. Tildesley, Computer Simulations of Liquids, Oxford University Press, Oxford, 1989.
[2] W.F. van Gunsteren, H.J.C. Berendsen, Angew. Chem., Int. Ed. Engl. 29 (1990) 992–1023.
[3] S.A. Rice, M. Zhao, Optical Control of Molecular Dynamics, Wiley, New York, 2000.
[4] M. Shapiro, P. Brumer, Principles of Quantum Control of Molecular Processes, Wiley, New York, 2003.
[5] T.C. Weinacht, P.H. Bucksbaum, J. Opt. B: Quant. Semiclass. Opt. 4 (2003) R35–R52.
[6] D. Goswami, Phys. Rep. 374 (2003) 385–481.
[7] T. Brixner, G. Gerber, Chem. Phys. Chem. 4 (2003) 418–438.
[8] M. Wollenhaupt, A. Assion, T. Baumert, in: F. Träger (Ed.), Spinger Handbook of Optics, Springer, New York, 2005.
[9] M. Born, E. Wolf, Principles of Optics, 6th ed., Cambridge University Press, Cambridge, 1997.
[10] R. Kosloff, A.D. Hammerich, D.J. Tannor, Phys. Rev. Lett. 69 (1992) 2172–2175.
[11] D. Tannor, in: A.D. Bandrauk (Ed.), Molecules in Laser Fields, Marcel Dekker, New York, 1994.
[12] V. Malinovsky, C. Meier, D.J. Tannor, Chem. Phys. 221 (1997) 67–76.
[13] V. Malinovsky, D.J. Tannor, Phys. Rev. A 56 (1997) 4929–4937.
[14] S. Gräfe, P. Marquetand, N.E. Henriksen, K.B. Møller, V. Engel, Chem. Phys. Lett. 398 (2004) 180–185.
[15] S. Gräfe, C. Meier, V. Engel, J. Chem. Phys. 122 (2005) 184103.
[16] P. Gross, H. Singh, H. Rabitz, K. Mease, G.M. Huang, Phys. Rev. A 47 (1993) 4593–4604.
[17] Y. Chen, P. Gross, V. Ramakrishna, H. Rabitz, J. Chem. Phys. 102 (1995) 8001–8010.
[18] V. May, O. Kühn, Charge and Energy Transfer Dynamics in Molecular Systems, Wiley–VCH, Berlin, 2000.
[19] S. Lochbrunner, E. Riedle, Rec. Res. Dev. Chem. Phys. 4 (2003) 31–61.
[20] E.T.J. Nibbering, T. Elsaesser, Chem. Rev. 104 (2004) 1887–1914.
[21] V. Engel, R. Schinke, V. Staemmler, Chem. Phys. 88 (1988) 129–148.
[22] V. Engel, V. Staemmler, R.L.V. Wal, F.F. Crim, R.J. Sension, B. Hudson, P. Andresen, S. Hennig, K. Weide, R. Schinke, J. Phys. Chem. 96 (1992) 3201–3213.
[23] B. Armstrup, N.E. Henriksen, J. Chem. Phys. 97 (1992) 8285–8295.
[24] N. Elgobashi, P. Krause, J. Manz, M. Oppel, Phys. Chem. Chem. Phys. 5 (2003) 4806–4813.
[25] J.R. Reimers, R.O. Watts, Mol. Phys. 52 (1984) 357–381.
[26] J. Zhang, D.G. Imre, J.H. Frederick, J. Phys. Chem. 93 (1989) 1840–1851.
[27] R. Schinke, Photodissociation Dynamics, Cambridge University Press, Cambridge, 1993.
[28] P.A.M. Dirac, The Principles of Quantum Mechanics, 4th ed., Oxford Science Publications, Oxford, 1958.
[29] P. Marquetand, S. Gräfe, D. Scheidel, V. Engel, J. Chem. Phys. 124 (2006) 054325.
[30] R.S. Judson, H. Rabitz, Phys. Rev. Lett. 68 (1992) 1500–1503.
[31] C.J. Bardeen, V.V. Yakovlevi, K.R. Wilson, S.D. Carpenter, P.M. Weber, W.S. Warren, Chem. Phys. Lett. 280 (1997) 151–158.
[32] A. Assion, T. Baumert, M. Bergt, T. Brixner, V. Seyfried, M. Strehle, G. Gerber, Science 282 (1998) 919–922.
[33] D. Meshulach, Y. Silberberg, Nature 396 (1998) 239–242.
[34] N. Dudovich, D. Oron, Y. Silberberg, Phys. Rev. Lett. 88 (2002) 123004.
[35] D. Zeidler, S. Frey, W. Wohlleben, M. Motzkus, F. Busch, T. Chen, W. Kiefer, A. Materny, J. Chem. Phys. 116 (2002) 5231–5235.
[36] J.L. Herek, W. Wohlleben, R. Cogdell, D. Zeidler, M. Motzkus, Nature 417 (2002) 533–535.
[37] C. Daniel, J. Full, L. Gonzalez, C. Lupulescu, J. Manz, A. Merli, S. Vajda, L. Wöste, Science 299 (2003) 536–539.
[38] M. Wollenhaupt, A. Präkelt, C. Sarpe-Tudoran, D. Liese, T. Baumert, J. Opt. B: Quant. Semiclass. Opt. 7 (2005) S1–S7.
[39] M. Dantus, V.V. Lozovoy, Chem. Rev. 104 (2004) 1813–1859.
[40] C. Cohen-Tannoudji, B. Diu, R. Laloë, Quantum Mechanics, vol. I, Wiley, New York, 1977.
[41] Y. Zhao, O. Kühn, J. Phys. Chem. A 104 (2000) 4882–4888.
[42] S. Chelkowski, A.D. Bandrauk, P.B. Corkum, Phys. Rev. Lett. 65 (1990) 2355–2358.
[43] T. Witte, T. Hornung, L. Windhorn, D. Proch, R. de Vivie-Riedle, M. Motzkus, K.L. Kompa, J. Chem. Phys. 118 (2003) 2021–2024.